

## Model of concentration changes across the synaptic cleft during a single quantum release

A. I. Skorinkin<sup>1,2</sup>, A. R. Shaihutdinova<sup>2,5</sup> and F. Vyskočil<sup>3,4</sup>

<sup>1</sup> *Institute of Physics, Kazan State University, Kremliovskaja ul. 18, 420008 Kazan, Russia. E-mail: askorink@yandex.ru*

<sup>2</sup> *Kazan Institute of Biochemistry and Biophysics, Russian Academy of Sciences, P.O.Box 30, 420111 Kazan, Russia*

<sup>3</sup> *Institute of Physiology, Czech Academy of Sciences, Vídeňská 1083, 142 20 Prague 4, Czech Republic*

<sup>4</sup> *Faculty of Science, Charles University, Viničná 7, 120 00 Prague, Czech Republic*

<sup>5</sup> *Kazan State Medical University, ul. Butlerova 49, 420012 Kazan, Russia*

**Abstract.** A model of concentration changes across the synaptic cleft during a single quantum release is presented that can be used for description and characterization of the kinetic in postsynaptic current development under the influence of different antagonists, modulators, desensitization promoters or complex channel blockers. The model enables the calculation of the relative number of open channels as a function of time for two standard cases – when acetylcholinesterase (AChE) is either active or inhibited. One outcome of the present model is that the variable part of AChE activity is zero at the moment of acetylcholine (ACh) release and then increases. This is in contrast to common view that the activity of AChE at the initial moment of release of quanta is maximal and decreases over the time course of quantum action. However, the model explains why non-quantal ACh leakage from the nerve terminal creating a concentration of approximately  $10^{-8}$  mol·l<sup>-1</sup> in the cleft can escape hydrolysis by intrasynaptically located cholinesterase and reach the subsynaptic membrane. The model can also be used for theoretical considerations of time and amplitude changes during repetitive nerve-evoked quanta release.

**Key words:** Release of quanta — Acetylcholine — Acetylcholinesterase — Model synapse

### Introduction

In recent years, neuromuscular synaptic transmission has not only been studied *via* a range of experimental procedures, but also with the help of mathematical simulation. Some models can describe and even predict the time course of acetylcholine (ACh) quanta release and its action on receptors with a reasonable degree of accuracy, as well as transmitter destruction by acetylcholinesterase (AChE) (Wathey et al. 1979; Nigmatullin et al. 1988; Snetkov et al. 1989; Friboulet and Thomas 1993; Stiles et al. 1996, 2000). However, it is often difficult to use these models in the description of multiquantal (up to 500 quanta)

postsynaptic current responses or to describe a prolonged series of single quantum responses, since they require large computational apparatus and extensive experimental data, which is often not available for a particular type of endplate. In this paper, a model is presented that can be used for such purposes.

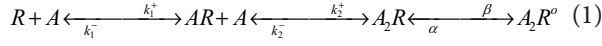
### Methods

#### *Description of the model*

It is generally accepted that at the motor endplate the diffusion of ACh through the synaptic cleft does not significantly affect the time course of postsynaptic unitary currents elicited by a single quantum, released from either the nerve or from artificial vesicles (Parnas et al. 1989), so it seems possible to consider, as an initial approximation, that the

Correspondence to: František Vyskočil, Institute of Physiology, Czech Academy of Sciences, Vídeňská 1083, 142 20 Prague 4, Czech Republic  
E-mail: vyskocil@biomed.cas.cz

concentration of ACh is identical at all points above the active postsynaptic zone at each moment. The activation of nicotinic ACh receptors (nAChR) is then described by the three-step kinetic diagram



where A – acetylcholine; AR – receptor with one molecule bound;  $A_2R$  – receptor with two molecules bound;  $A_2R^o$  – receptor with two molecules bound and an open channel;  $k_1^+$ ,  $k_1^-$ ,  $k_2^+$ ,  $k_2^-$ ,  $\beta$ ,  $\alpha$  – the rate constants of the corresponding reactions. The mathematical model of the processes indicated in this diagram includes three differential equations for the concentrations of receptors, which are in different states (Chretien and Chauvet 1998), and the equation of the conservation of the total number of receptors on the membrane

$$\begin{aligned} \frac{d[AR]}{dt} &= k_1^+ \cdot [R] \cdot [A] - k_1^- \cdot [AR] + k_2^- \cdot [A_2R] - k_2^+ \cdot [AR] \cdot [A] \\ \frac{d[A_2R]}{dt} &= \alpha \cdot [A_2R^o] - \beta \cdot [A_2R] - k_2^- \cdot [A_2R] + k_2^+ \cdot [AR] \cdot [A] \\ \frac{d[A_2R^o]}{dt} &= \beta \cdot [A_2R] - \alpha \cdot [A_2R^o] \\ [R] + [AR] + [A_2R] + [A_2R^o] &= [R_o] \end{aligned} \quad (2)$$

It is more convenient to operate with this scheme, if each equation is divided by the total concentration of receptors and to designate the relative quantities of receptors in the various states as  $[R]/[R_o] = r$ ,  $[AR]/[R_o] = x$ ,  $[A_2R]/[R_o] = y$ ,  $[A_2R^o]/[R_o] = z$ . The total system scheme can then be written down in the form:

$$\begin{aligned} \frac{dx}{dt} &= k_1^+ \cdot r \cdot [A] - k_1^- \cdot x + k_2^- \cdot y - k_2^+ \cdot x \cdot [A] \\ \frac{dy}{dt} &= \alpha \cdot z - \beta \cdot y - k_2^- \cdot y + k_2^+ \cdot x \cdot [A] \\ \frac{dz}{dt} &= \beta \cdot y - \alpha \cdot z \\ r + x + y + z &= 1 \end{aligned} \quad (3)$$

Furthermore, it is possible to extract a separate differential equation for the concentration of ACh

$$\begin{aligned} \frac{d[A]}{dt} &= w(t) - p \cdot [A] - f(t) \cdot [A] + k_1^- \cdot [AR] + k_2^- \cdot [A_2R] - \\ &\quad - k_1^+ \cdot [A] \cdot [R] - k_2^+ \cdot [A] \cdot [AR] \end{aligned} \quad (4)$$

where  $w(t)$  – rate of ACh quantum release from the nerve terminal,  $p$  – coefficient which determines the rate of ACh outflow from the cleft due to diffusion and the possible reuptake of choline by the nerve terminal (and all possible another ways of ACh inactivation, including the constant part of AChE activity),  $f(t)$  – variable part of the rate of ACh hydrolysis with cholinesterase.

## Results

It is worth noting that the process of the release of quanta from presynaptic nerve terminals can vary in the synapses of different animals or even in the same synapses under different physiological conditions (awake and hibernating hamsters, Moravec and Vyskočil 2005) and it is therefore necessary to select the most thoroughly and most precisely defined parameters for further calculation and simulation. All results described in this article are based on experimental data obtained from the neuromuscular preparation of frog *Rana ridibunda* using a standard two-electrode voltage clamp method. The reaction rate constants for nAChR were also taken from the work of Stiles et al. (1999) ( $k_1^+ = 160.6 \text{ mmol} \cdot \text{l}^{-1} \cdot \text{ms}^{-1}$ ,  $k_1^- = 18.4 \text{ ms}^{-1}$ ,  $k_2^+ = 80.3 \text{ mmol} \cdot \text{l}^{-1} \cdot \text{ms}^{-1}$ ,  $k_2^- = 36.8 \text{ ms}^{-1}$ ,  $\beta = 36.7 \text{ ms}^{-1}$ ,  $\alpha = 1.7 \text{ ms}^{-1}$ ). Our model enables the calculation of the relative number of open channels as a function of time for two standard cases – when AChE is either active or inhibited, and these calculated values are in agreement with experimentally recorded postsynaptic currents  $I(t)$  flowing through an nAChR channel opened by one quantum of ACh: for both cases  $z(t) = N \cdot I(t)/I_o$ , where  $N$  – maximum relative fraction of channels opened simultaneously,  $I_o$  – amplitude of the membrane current. Available experimental data enables the evaluation of  $N = I_o/(R_o \cdot \gamma \cdot U)$ , which is 0.6 when cholinesterase is active and 0.85 when it is inhibited (Fig. 1). These calculations were based on total number of receptors in the active zone  $R_o \approx 5000$  (Lester et al. 1978; Matthews-Bellinger and Salpeter 1978; Salpeter et al. 1984), amplitude of the current  $I_o \approx 7.5 \text{ nA}$  with active AChE and  $I_o \approx 10.5 \text{ nA}$  with inhibited AChE at the holding

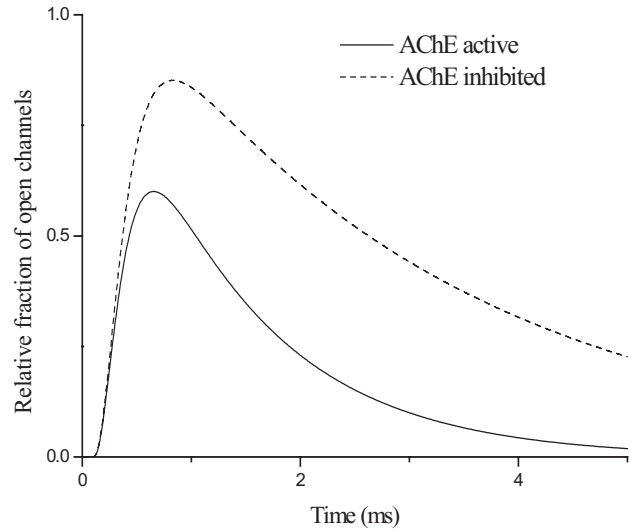


**Figure 1.** Change in the relative number of open channels during the release of single quanta of ACh; reconstruction of experimental data. AChE, acetylcholinesterase.

membrane potential  $-100$  mV (Land et al. 1984; Adams 1989; Bartol et al. 1991) and the conductivity of a single nAChR channel  $\gamma \approx 25$  pS (Colquhoun 1981).

From these experimental data, the function of  $z(t)$  was then obtained as:

$$z(t) = 1.12 \cdot \left(1 - e^{-\frac{t}{0.2}}\right)^{2.5} \cdot e^{-\frac{t}{1.2}} \quad (5)$$

provided that AChE was active and

$$z(t) = 1.16 \cdot \left(1 - e^{-\frac{t}{0.2}}\right)^{2.5} \cdot e^{-\frac{t}{3.0}} \quad (6)$$

provided that AChE was inhibited.

Their first derivatives against time were expressed as:

$$\frac{dz}{dt} = 14.0 \cdot \left(1 - e^{-\frac{t}{0.2}}\right)^{1.5} \cdot e^{-\frac{t}{1.2}} \cdot e^{-\frac{t}{0.2}} - 0.933 \cdot \left(1 - e^{-\frac{t}{0.2}}\right)^{2.5} \cdot e^{-\frac{t}{1.2}} \quad (7)$$

provided that AChE was active and

$$\frac{dz}{dt} = 14.5 \cdot \left(1 - e^{-\frac{t}{0.2}}\right)^{1.5} \cdot e^{-\frac{t}{3.0}} \cdot e^{-\frac{t}{0.2}} - 0.387 \cdot \left(1 - e^{-\frac{t}{0.2}}\right)^{2.5} \cdot e^{-\frac{t}{3.0}} \quad (8)$$

provided that AChE was inhibited.

This could then be substituted into the third equation of system (3) to find  $y(t)$ .

$$y(t) = \frac{\alpha}{\beta} \cdot z(t) + \frac{1}{\beta} \cdot \frac{dz(t)}{dt} \quad (9)$$

After this, it was also possible to numerically find  $\frac{dy(t)}{dt}$ , to express  $r(t) = 1 - x(t) - y(t) - z(t)$ , from the last equation of system (3) and obtain  $[A](t, x(t))$  from the second equation in the same system (3)

$$[A](t, x(t)) = \frac{1}{k_2^+ \cdot x(t)} \cdot \frac{dy(t)}{dt} - \frac{\alpha \cdot z(t)}{k_2^+ \cdot x(t)} + \frac{\beta \cdot y(t)}{k_2^+ \cdot x(t)} + \frac{k_2^- \cdot y(t)}{k_2^+ \cdot x(t)} \quad (10)$$

After substituting all these results into the first equation of system (3), it was possible to solve (in this case the fourth order Runge–Kutta method was used) for  $x(t)$  and, after substituting that  $x(t)$  into Eq. (10), find  $A(t)$ . The last function for both active and inhibited AChE is given in Fig. 2. It is interesting to note that the calculated peak concentration of ACh was found in the range  $0.15$ – $0.30$   $\text{mmol} \cdot \text{l}^{-1}$ , and this corresponds well with known literature data (Hartzell et al. 1975; Lester et al. 1978; Matthews-Bellinger and Salpeter 1978).

The solution of separate differential Eq. (4) for the concentration of ACh for both active and inhibited AChE made it possible to also reproduce the rate of the release of ACh quanta from presynaptic nerve terminals and the function of the activity of AChE. The function of quanta release can be determined from the equation:

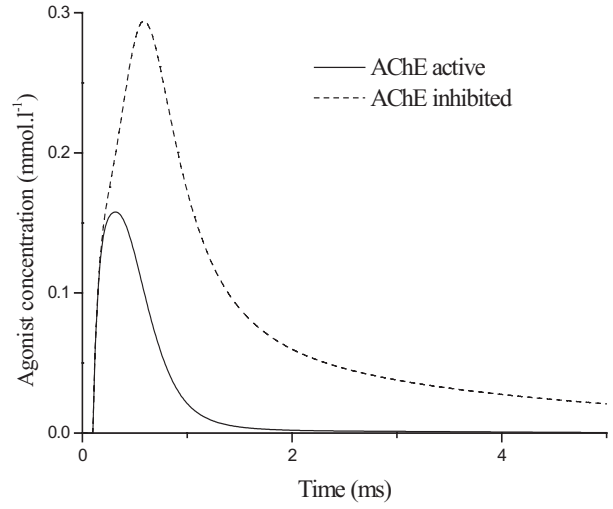


**Figure 2.** Change in ACh concentration ( $\text{mmol/l}$ ) in synaptic cleft during release of single quanta; kinetic calculation data. AChE, acetylcholinesterase.

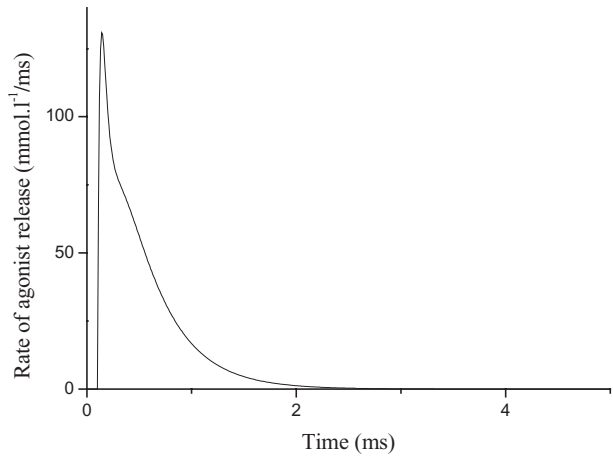


**Figure 3.** Rate of ACh quanta release into synaptic cleft; kinetic calculation data.

$$w(t) = \frac{d[A^i]}{dt} + p \cdot [A^i] - k_1^- \cdot [AR^i] - k_2^- \cdot [A_2R^i] + k_1^+ \cdot [A^i] \cdot [R^i] + k_2^+ \cdot [A^i] \cdot [AR^i] \quad (11)$$

where the value of coefficient  $p$  ( $120 \text{ ms}^{-1}$ ) was selected to give the minimum (obligatorily non-negative) release of quanta, and the superscript  $i$  indicates that all values are taken for inhibited AChE. The obtained curve is well approximated by the equation:

$$w(t) = 3200 \cdot \left(1 - e^{-\frac{t}{0.4}}\right) \cdot e^{-\frac{t}{0.035}} + 174 \cdot \left(1 - e^{-\frac{t}{0.165}}\right) \cdot e^{-\frac{t}{0.385}} \quad (12)$$

where the rate of release of quanta is expressed in  $\text{mmol} \cdot \text{l}^{-1} \cdot \text{ms}^{-1}$ , time in ms; this approximation is given in Fig. 3.

It is worth noting two rather complicated issues that arose during the estimation of the function  $w(t)$ . First, the inhibition of AChE by any drug is far from complete (Giacobini 2000); therefore  $f(t)$  should be considered to only be a variable part of the cholinesterase activity, and the part of AChE that remains still active in the presence of anticholinesterases becomes part of coefficient  $p$ .

Secondly, the absolute concentrations of different states of receptors are used in Eq. (4) in contrast to their relative quantities used in system (3); reliable estimations of nAChRs on the postsynaptic membrane in the active zone of the release are available and the surface density in the zone facing the site of quanta release is about 40,000 *per* square micrometer (Stiles et al. 1996, 2000). If we consider that the surface of the membrane is a section of the volume uniformly filled with receptors, then the concentration of receptors can be determined according to the equation

$$[R_o] = \frac{(\sqrt{d})^3}{N_A} \cdot 10^{18} \quad (13)$$

where  $[R_o]$  – concentration of receptors in  $\text{mmol}\cdot\text{l}^{-1}$ ,  $N_A$  – the Avogadro number,  $d$  – surface density in  $1\ \mu\text{m}^{-2}$ , then  $[R_o] \approx 14\ \text{mmol}\cdot\text{l}^{-1}$ . The function of the variable part of the AChE activity of can be determined from the equation:

$$f(t) = \frac{w(t) - p \cdot [A^a] + k_1^- \cdot [AR^a] + k_2^- \cdot [A_2R^a] - k_1^+ \cdot [A^a] \cdot [R^a] - k_2^+ \cdot [A^a] \cdot [AR^a] - \frac{d[A^a]}{dt}}{[A^a]} \quad (14)$$

where superscript *a* indicates that all values are taken for active AChE. The obtained curve is approximated well by the equation

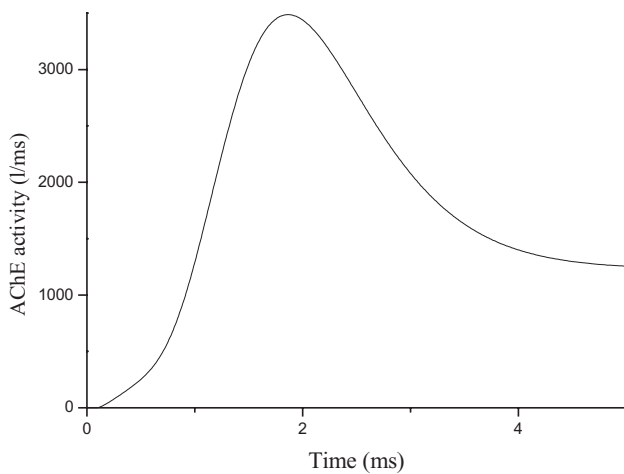


**Figure 4.** Change in activity of acetylcholinesterase (AChE) in synaptic cleft during the release of single quanta of ACh; kinetic calculation data.

$$f(t) = 207000 \cdot \left(1 - e^{-\frac{t}{0.89}}\right)^9 \cdot e^{-\frac{t}{0.58}} + 1240 \cdot \left(1 - e^{-\frac{t}{1.2}}\right)^{1.3} \quad (15)$$

where the activity of AChE is expressed in  $\text{ms}^{-1}$ , time in ms (Fig. 4).

If we now substitute the approximated functions of  $w(t)$  and  $f(t)$  into Eq. (4) and solve it together with system (3), then the calculated values of  $z(t)$  (Fig. 5) are very similar to experimentally obtained curves (Fig. 1).

## Discussion

A rather unexpected outcome of the present model is that  $f(t)$ , i.e. the variable part of cholinesterase activity, is zero at the moment of quanta release and then increases (cf. Figs. 2 and 3); usually the activity of AChE at the initial moment of release of quanta is considered to be maximal in this type of model and decreases over the time course of quanta activity (Rosenberry 1979; Nigmatullin et al. 1988; Snetkov et al. 1989).

How can this initial cholinesterase inactivity be explained? There might be a substrate inhibition of the enzyme by the ACh quantum dose that can delay the ACh hydrolysis. Further, there are indications that a major part of the AChE is located in the synaptic folds and only becomes active after the released ACh reaches these sites (Anglister et al. 1994). But still, at least one third of the ACh molecules are hydrolyzed even before they reach the nAChR, as indicated by the size of the maximal amplitude of the miniature endplate currents before and after cholinesterase inhibition (Deana and Scuka 1990; Giniatullin et al. 2001). Another explanation is biochemical. AChE might not be sufficiently activated

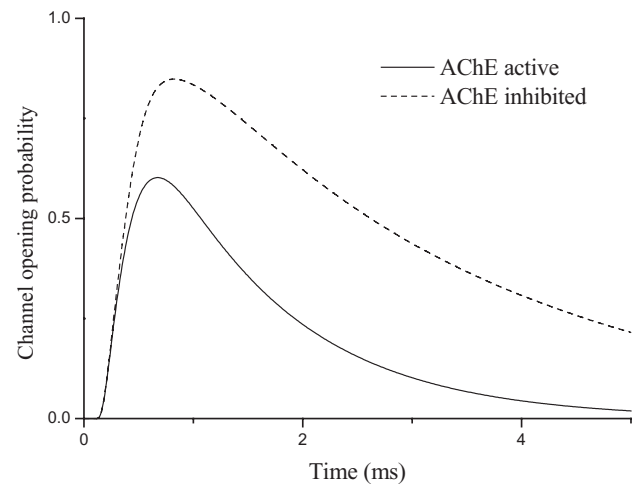


**Figure 5.** Change in relative number of open channels during single quanta release; kinetic calculation data. AChE, acetylcholinesterase.

by the initial low ACh concentration at the beginning of the quanta release indicated by gradual rise phase of unquantal postsynaptic currents (e.g. Giniatullin et al. 2001). The comparison of initial phases of the curves on Figs. 2 and 3 indicates the beginning of ACh hydrolysis when its concentration is  $>100 \mu\text{mol}\cdot\text{l}^{-1}$ . This idea seems to be in accord with the classical experiments of Augustinsson (1946), who showed that the velocity of hydrolysis of ACh by AChE decreases sharply when the concentration of ACh is less than  $10^{-4} \text{ mol}\cdot\text{l}^{-1}$  (cf. also Cohen and Hagen 1964; Ecobichon and Israel 1967). Each catalytic subunit of AChE has two allosterically regulated ACh binding sites, which have to be occupied simultaneously for full activation, and this only occurs when ACh reaches high concentrations (Taylor 1991). Moreover, the enzyme is fixed at the basal lamina and this provides an opportunity for a definite number of free ACh molecules to bypass the enzyme and reach the subsynaptic membrane. Also, the non-quantal ACh in rodents, i.e. a small but continuous ACh leakage from the nerve terminal creating a concentration of approximately  $10^{-8} \text{ mol}\cdot\text{l}^{-1}$  in the cleft (Vyskočil et al. 1983), can escape hydrolysis by intrasynaptically located cholinesterase and reach the subsynaptic membrane. This even activates electrogenic Na,K-ATPase and creates the small, but obvious, “surplus” hyperpolarization (by 2–4 mV) in the resting membrane potential in the endplate zone (Thesleff et al. 1974; Vyskočil 1974).

This model definitely has certain limitations; since it does not consider the distance between the ACh molecule release site and particular receptor, it evidently cannot be used in situations where processes of diffusion might be of relevant importance, such as desensitization-caused or irreversible antagonist-induced “pruning” of receptors *versus* the endplate current duration. However, this model can accurately describe and characterize the kinetic constants and corresponding changes in postsynaptic current development under the influence of different antagonists, modulators, desensitization promoters or complex channel blockers. It can also be used for modeling time and amplitude changes during repetitive ( $<100$  Hz) nerve-evoked quanta release.

**Acknowledgements.** This work was supported by the “Leading Scientific School” grant of the Russian Federation, RFBR grants (A. I. S. and A. R. S), GAAVA5011411, GAČR202/02/1213 and AV0Z 5011050922 (F. V.).

## References

- Adams B. A. (1989): Temperature and synaptic efficacy in frog skeletal muscle. *J. Physiol. (Lond.)* **408**, 443–455
- Anglister L., Stiles J. R., Salpeter M. M. (1994): Acetylcholinesterase density and turnover number at frog neuromuscular junctions, with modeling of their role in synaptic function. *Neuron* **12**, 783–794
- Augustinsson K. B. (1946): Studies on the specificity of choline esterase in *Helix pomatia*. *Biochem. J.* **40**, 343–349
- Bartol T. M., Land B. R., Salpeter E. E., Salpeter M. M. (1991): Monte Carlo simulation of miniature endplate current generation in the vertebrate neuromuscular junction. *Biophys. J.* **59**, 1290–1307
- Chretien J. M., Chauvet G. A. (1998): An algorithmic method for determining the kinetic system of receptor-channel complexes. *Math. Biosci.* **14**, 227–257
- Cohen L. H., Hagen P. B. (1964): A physiological role for the pre-synaptic localization of acetylcholinesterase and for its inhibition by excess substrate. *Can. J. Biochem. Physiol.* **42**, 593–594
- Colquhoun D. (1981): *Drug Receptors and Their Effectors*. pp. 107–127, Macmillan, London
- Deana A., Scuka M. (1990): Time course of neostigmine action on the endplate response. *Neurosci. Lett.* **118**, 82–84
- Ecobichon D. J., Israel Y. (1967): Characterization of the esterases from electric tissue of *Electrophorus* by starch-gel electrophoresis. *Can. J. Biochem.* **45**, 1099–1105
- Friboulet A., Thomas D. (1993): Reaction-diffusion coupling in a structured system: application to the quantitative simulation of endplate currents. *J. Theor. Biol.* **160**, 441–455
- Giacobini E. (2000): Cholinesterase inhibitors stabilize Alzheimer disease. *Neurochem. Res.* **25**, 1185–1190
- Giniatullin R. A., Talantova M. V., Vyskočil F. (2001): The role of desensitisation in decay time of miniature endplate currents in frogs *Rana ridibunda* and *Rana temporaria*. *Neurosci. Res.* **39**, 287–292
- Hartzell H. C., Kuffler S. W., Yoshikami D. (1975): Post-synaptic potentiation: interaction between quanta of acetylcholine at the skeletal neuromuscular synapse. *J. Physiol. (Lond.)* **251**, 427–463
- Land B. R., Harris V. W., Salpeter E. E., Salpeter M. M. (1984): Diffusion and binding constants for acetylcholine derived from the falling phase of miniature endplate currents. *Proc. Natl. Acad. Sci. U.S.A.* **81**, 1594–1598
- Lester H. A., Koblin D. D., Sheridan R. E. (1978): Role of voltage-sensitive receptors in nicotinic transmission. *Biophys. J.* **21**, 181–194
- Mattews-Bellinger J., Salpeter M. M. (1978): Distribution of acetylcholine receptors at frog neuromuscular junctions with a discussion of some physiological implications. *J. Physiol. (Lond.)* **279**, 197–213
- Moravec J., Vyskočil F. (2005): Early postdenervation depolarization develops faster at endplates of hibernating golden hamsters where spontaneous quantal and non-quantal acetylcholine release is very small. *Neurosci. Res.* **51**, 25–29
- Nigmatullin N. R., Snetkov V. A., Nikol'skii E. E., Magazanik L. G. (1988): Analysis of a model of the miniature endplate current. *Neirofiziologiya* **20**, 390–398 (in Russian)
- Parnas H., Flashner M., Spira M. E. (1989): Sequential model to describe the nicotinic synaptic current. *Biophys. J.* **55**, 875–884
- Rosenberry T. L. (1979): Quantitative simulation of endplate currents at neuromuscular junctions based on the reaction

- of acetylcholine with acetylcholine receptor and acetylcholinesterase. *Biophys. J.* **26**, 263–289
- Salpeter M. M., Smith C. D., Matthews-Bellinger J. A. (1984): Acetylcholine receptor at neuromuscular junctions by EM autoradiography using mask analysis and linear sources. *J. Electron Microsc. Tech.* **1**, 63–81
- Snetkov V. A., Nigmatullin N. R., Nikol'skii E. E., Magazanik L. G. (1989): Simulation of the action of ion channel blockaders on post-synaptic currents. *Neirofiziologiya* **21**, 476–484 (in Russian)
- Stiles J. R., Van Helden D., Bartol T. M., Salpeter E. E., Salpeter M. M. (1996): Miniature endplate current rise times less than 100 microseconds from improved dual recordings can be modeled with passive acetylcholine diffusion from a synaptic vesicle. *Proc. Natl. Acad. Sci. U.S.A.* **93**, 5747–5752
- Stiles J. R., Kovyazina I. V., Salpeter E. E., Salpeter M. M. (1999): The temperature sensitivity of miniature endplate currents is mostly governed by channel gating: evidence from optimized recordings and Monte Carlo simulations. *Biophys. J.* **77**, 1177–1187
- Stiles J. R., Bartol T. M. Jr., Salpeter M. M., Salpeter E. E., Sejnowski T. J. (2000): Synaptic variability: new insights from reconstructions and Monte Carlo simulation. In: *Synapses*. pp. 681–727, Johns Hopkins University Press, Baltimore, London
- Taylor P. (1991): The cholinesterases. *J. Biol. Chem.* **6**, 4025–4028
- Thesleff S., Vyskočil F., Ward W. R. (1974): The action potential in end-plate and extrajunctional regions of rat skeletal muscle. *Acta Physiol. Scand.* **91**, 196–202
- Vyskočil F., Nikolsky E., Edwards C. (1983): An analysis of the mechanisms underlying the non-quantal release of acetylcholine at the mouse neuromuscular junction. *Neuroscience* **9**, 429–435
- Vyskočil F. (1974): Action potentials of the rat diaphragm and their sensitivity to tetrodotoxin during postnatal development and old age. *Pflügers Arch.* **352**, 155–163
- Wathey J. C., Nass M. N., Lester H. A. (1979): Numerical reconstruction of the quantal event at nicotinic synapses. *Biophys. J.* **27**, 145–164

Final version accepted: October 22, 2007